

## Dynamics of a Bouncing Droplet onto a Vertically Vibrated Interface

T. Gilet,<sup>\*</sup> D. Terwagne, N. Vandewalle, and S. Dorbolo<sup>†</sup>

<sup>1</sup>GRASP, Physics Department B5a, University of Liège, B-4000 Liège, Belgium

(Received 9 November 2007; published 23 April 2008)

Low viscosity ( $< 100$  cSt) silicon oil droplets are placed on a high viscosity (1000 cSt) oil bath that vibrates vertically. The viscosity difference ensures that the droplet is more deformed than the bath interface. Droplets bounce periodically on the bath when the acceleration of its sinusoidal motion is larger than a threshold value. The threshold is minimum for a particular frequency of excitation: droplet and bath motions are in resonance. The bouncing droplet has been modeled by considering the deformation of the droplet and the lubrication force exerted by the air layer between the droplet and the bath. Threshold values are predicted and found to be in good agreement with our measurements.

DOI: [10.1103/PhysRevLett.100.167802](https://doi.org/10.1103/PhysRevLett.100.167802)

PACS numbers: 68.15.+e, 47.55.D-, 68.03.Cd

The manipulation of individual droplets becomes progressively more important in microfluidics, as it is a promising alternative to fluid displacement in micro-channels [1,2]. A droplet may be considered as a micro-scale chemical reactor with a high efficiency [3] or as a variable focus optical lens [4]. When a droplet is laid on a liquid bath, its coalescence with the bath often takes a short time since the air layer separating the droplet from the bath has to be drained out. This drainage may be delayed by vertically vibrating the bath [5]: the droplet bounces periodically without coalescing. With this experiment, a droplet may be manipulated without any contact with a solid element, which minimizes the chemical contamination. The manipulation of bouncing droplets is straightforward: droplets move spontaneously by interacting with the wave they produce on the bath at each impact [6]. By using this wave, they probe the surroundings and detect the presence of other droplets or solid obstacles, they may be guided [7]. Several droplets on the same bath interact together and experience orbital motions [6] or form 2D crystalline lattices [8]. Finally, partial coalescence allows low viscosity droplets to be emptied step-by-step. This emptying cascade stops when droplets are able to bounce periodically [9].

Couder *et al.* [5] investigated the bouncing of an homogeneous system: the droplet and the bath are made with the same viscous oil (500 cSt). The vertical position of the vibrated bath is given by  $A \cos(2\pi ft)$ , where  $A$  and  $f$  are the forcing amplitude and frequency, respectively. The reduced acceleration  $\Gamma$  is defined as  $\Gamma = 4\pi^2 A f^2 / g$ . Periodic bouncing is observed when  $\Gamma$  is higher than a critical value  $\Gamma_C$ , the threshold for bouncing. Couder *et al.* observed that  $\Gamma_C - 1 \sim f^2$  and explained this scaling by balancing the gravity, the inertial forces, and the lubrication force exerted on the droplet by the squeezed air layer. Deformations of both the droplet and the bath were not considered.

Bouncing mechanisms of liquid objects have been studied in a wide range of configurations: a droplet bounc-

ing on a hydrophobic solid surface [10] or on an horizontal wall immersed into an immiscible liquid [11], a bubble bouncing on a water/air interface [12].... As in elastic solids, the deformation of those liquid objects is often the key ingredient that ensures the bouncing property, due to surface tension. Deformations may be significantly damped by viscous effects when the Ohnesorge number  $Oh = \nu \sqrt{\rho / \sigma R}$  is larger than unity, where  $R$  is the droplet radius and  $\rho$ ,  $\nu$ , and  $\sigma$  are the density, the viscosity, and the surface tension of the liquid, respectively. In the experiment of Couder,  $Oh \sim 4$ , which means that deformations may be neglected.

In this Letter, we investigate the bouncing of low viscosity droplets, for which the deformation is important ( $Oh \ll 1$ ). The scaling law proposed by Couder [5] for the threshold acceleration is not valid anymore: values of  $\Gamma_C$  below unity have been observed [7,9]. In order to focus on the droplet deformation, we analyze the bouncing of low viscosity droplets (1.5 to 100 cSt) on a high viscosity bath (1000 cSt): the system is inhomogeneous, and the deformation of the bath surface is much smaller than the droplet deformation. First, we measure  $\Gamma_C$  for various  $\nu$  and  $f$  with  $R$  fixed. Then, a model that incorporates both the droplet deformation and the lubrication force is developed.

A container filled with 1000 cSt silicon oil is fixed on a vertically vibrating electromagnetic shaker. By using a syringe, droplets of radius  $R = 0.765$  mm with viscosities of 1.5, 10, 50, and 100 cSt are placed on the bath. Measured threshold accelerations  $\Gamma_C$  are shown in Fig. 1. The threshold is determined by using two different protocols. First, the droplet is created when the acceleration is sufficiently high for bouncing to occur. The forcing amplitude is then slowly decreased ( $f$  fixed) until the droplet stops bouncing and coalesces with the bath (● in Fig. 1). Then, starting from zero,  $\Gamma$  is increased. After each increment, a droplet is laid on the surface of the bath. When this droplet bounces, the threshold is reached (▲ in Fig. 1). An hysteresis, i.e., a difference in  $\Gamma_C$  deduced by both methods, is observed for

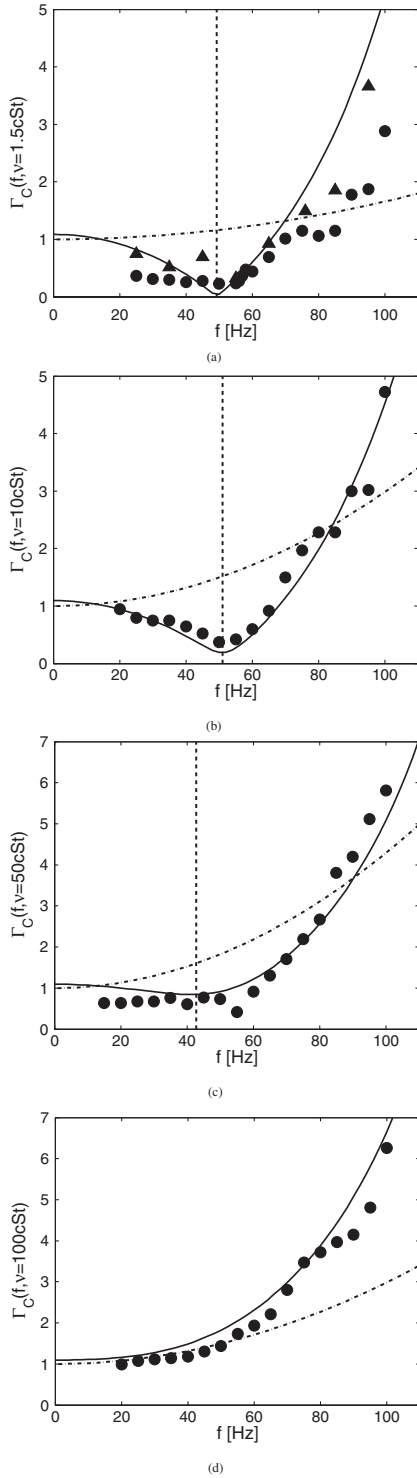


FIG. 1. Acceleration threshold  $\Gamma_C$  for various viscosities of the droplet: (a)  $\nu = 1.5$  cSt, (b)  $\nu = 10$  cSt, (c)  $\nu = 50$  cSt, and (d)  $\nu = 100$  cSt. For  $\nu = 1.5$  cSt, thresholds are different according to whether the acceleration is increased ( $\blacktriangle$ ) or decreased ( $\bullet$ ). The solid line corresponds to the model prediction [Eq. (9)], with coefficients given in Table I. The dash-dot line is a fit by the scaling of Couder ( $\Gamma_C - 1 \sim f^2$ ). The vertical dashed line enhances the resonance frequency  $\omega_{\text{res}}$  described in the model. Error bars correspond to the size of symbols.

$\nu = 1.5$  cSt [Fig. 1(a)]. For high viscosity droplets [Fig. 1(d)],  $\Gamma_C > 1$ , and  $\partial\Gamma_C/\partial f > 0$  as predicted in [5]. For lower droplet viscosities, the threshold may be lower than 1, and there is a minimum in the  $\Gamma_C(f)$  curve. At high frequency, this curve strongly increases with  $f$ .

The following model is proposed in order to describe the  $\Gamma_C$  dependence on the forcing frequency  $f$  and the droplet viscosity  $\nu$ . The flow is assumed to be axisymmetric and the motion of the droplet mass center (mass  $M$ ) confined to a vertical axis. The droplet bouncing is modeled with two scalar ordinary differential equations describing the vertical position  $x_c$  of the mass center and the vertical deformation  $\eta$  of the droplet (Fig. 2), respectively. The bath deformation is neglected. During its flight, the droplet experiences an apparent gravity  $Mg(\Gamma \cos 2\pi ft - 1)$  in a frame moving with the bath. Moreover, the droplet is stressed by the surrounding air, resulting in a vertical force  $F$ . The influence of air is negligible on the droplet movement, except when there is a thin air layer between the droplet and the bath surface. Then,  $F$  can be estimated by lubrication theory [13] and depends on the thickness  $h$  of the film and its rate of decrease  $\dot{h}$ . Movements inside the droplet also have a significant influence on the air film drainage. This latter can be modeled to leading order by a Poiseuille flow between two parallel planar interfaces. The bottom interface is at rest (the bath is static), while the upper moves with a vertical velocity equal to  $\dot{h}$  and a horizontal velocity proportional to  $\dot{\eta}r/R$ , where  $r$  is the radial cylindrical coordinate, and  $R$  the radius of the unstrained droplet. Therefore,

$$F = c_1 \mu_a R^4 \left( c_2 \frac{\dot{\eta}}{h^2 R} - \frac{\dot{h}}{h^3} \right) \quad (1)$$

where  $c_1, c_2$  are positive constants, and  $\mu_a$  is the dynamic

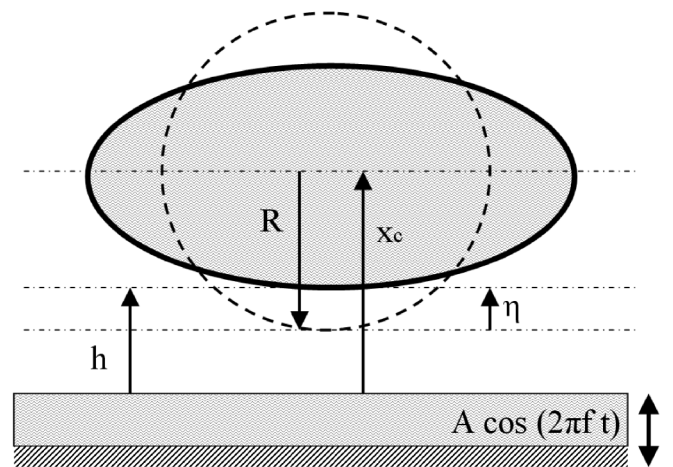


FIG. 2. Geometrical variables needed to model a bouncing droplet of undeformed radius  $R$ :  $x_c$  is the distance between the droplet center of mass and the bath,  $h$  is the minimum air film thickness, and  $\eta$  is the vertical droplet deformation about the axis of symmetry.

viscosity of the air. According to the lubrication theory,  $c_1 = 3\pi/2$ . The parameter  $c_2$  represents the influence of the flow inside the droplet on the flow in the air film. It cannot be estimated by simple arguments. Newton's second law applied to the droplet is written as

$$M \frac{d^2 x_c}{dt^2} = Mg(\Gamma \cos 2\pi f t - 1) + F. \quad (2)$$

For practical purposes, we use  $h = x_c - R - \eta$  instead of  $x_c$ . The evolution of  $\eta$  is prescribed by an energy balance in the frame of the mass center of the droplet:

$$\frac{d(K + E)}{dt} = -P_d - P_f \quad (3)$$

where  $K$  is the kinetic energy of the motion inside the droplet,  $E$  is the interfacial energy, and  $P_d$  is the viscous dissipative power inside the droplet. The power developed by  $F$ , called  $P_f$ , is supposed to be equal to  $c_6 \dot{\eta} F$ . A convenient way to estimate  $K$ ,  $E$ , and  $P_d$  as a function of  $\eta$  refers to the potential flow related to infinitesimal capillary waves at the surface of a droplet [14] (see Table I). The deformation  $\eta$  measured experimentally is less than 10% of the initial radius, which validates the linear approach [15]. We suppose that only the mode 2 is excited by the bouncing since higher modes have much higher resonance frequencies.

The whole system is written in dimensionless form by using  $R$  as a length scale and the capillary time  $\tau_\sigma = \sqrt{M/\sigma}$  as a time scale. Moreover, Eq. (3) is replaced by  $c_6$  times Eq. (2) plus  $1/\dot{\eta}$  times Eq. (3), in order to remove the lubrication term

$$\begin{aligned} \ddot{h} + \dot{\eta} &= \text{Bo}(\Gamma \cos \omega t - 1) + c_1 \frac{3\mu_a}{4\pi\nu\rho} \text{Oh} \left( c_2 \frac{\dot{\eta}}{h^2} - \frac{\dot{h}}{h^3} \right) \\ (c_3 + c_6)\dot{\eta} + c_5 \text{Oh} \dot{\eta} + c_4 \eta &= c_6 \text{Bo}(\Gamma \cos \omega t - 1) - c_6 \dot{h} \end{aligned} \quad (4)$$

where  $\text{Bo} = \frac{Mg}{\sigma R}$  is the Bond number and  $\omega = 2\pi f \tau_\sigma$  is the reduced frequency.

Terwagne *et al.* [16] observed the dynamics of the air film located between the droplet and the bath using a monochromatic light: concentric fringes of interference appear when the air film is squeezed. When the droplet

TABLE I. Constitutive laws for the energy balance of the droplet deformation. Second and third columns are theoretical coefficients  $c_i$  for modes 2 (spheroid) and 3, while the fourth column corresponds to the best fit of Eq. (9) on experimental data.

| Law                                  | Mode 2          | Mode 3          | Fit         |
|--------------------------------------|-----------------|-----------------|-------------|
| $K = c_3 M \dot{\eta}^2 / 2$         | $c_3 = 3/10$    | $c_3 = 1/7$     | $c_3 = 0.1$ |
| $E = c_4 \sigma \eta^2 / 2$          | $c_4 = 16\pi/5$ | $c_4 = 40\pi/7$ | $c_4 = 10$  |
| $P_d = c_5 \nu M \dot{\eta}^2 / R^2$ | $c_5 = 3$       | $c_5 = 4$       | $c_5 = 3.3$ |

bounces, the motion of the fringes is perfectly periodic: no attenuation or phase drift takes place and the bouncing is stationary. On the other hand, the number of fringes decreases when the droplet does not bounce: the film thins. The periodicity of the fringes motion suggests periodic solutions from Eq. (4). Conditions for such solutions are obtained by integrating Eq. (4) over a period  $T = 2\pi/\omega$ . Under the assumption of periodicity, many terms vanish, giving

$$\begin{aligned} - \int_0^T \eta dt &= \frac{c_6}{c_4} \text{Bo} T, \\ \int_0^T \frac{\dot{\eta}}{h^2} dt &= \frac{4\pi}{3c_1 c_2} \frac{\nu \rho}{\mu_a} \frac{\text{Bo} T}{\text{Oh}}. \end{aligned} \quad (5)$$

Terms on the right-hand side are always strictly positive. According to the first relation, a mechanism of potential energy storage (here, the droplet deformation) should be taken into account ( $\eta \neq 0$ ). The droplet has to spend more time in an oblate state ( $\eta < 0$ ) than in a prolate state ( $\eta > 0$ ). According to the second equation, internal movements in the liquid phase, related to the deformation rate, must have a significant influence on the film drainage and the resulting lubrication force. Moreover, a significant phase shift between the minimum film thickness and the maximum compression must be observed. Indeed,  $\int_0^T \dot{\eta} dt = 0$ , while  $1/h^2$  is strictly positive and vanishes when the film thickens. To have a positive left hand side in the second equation, we expect the film to be the thinnest when the droplet begins to recover its spherical shape ( $\dot{\eta} > 0$ ). All these required conditions show us that this model is minimal: if the model does not take into account all above listed conditions, its prediction fails, and no periodic bouncing solutions can be found.

The acceleration threshold  $\Gamma_C$  required for periodic bouncing may be estimated starting from Eq. (4). When  $\Gamma < \Gamma_C$ , the droplet does not bounce, the air film remains thin, and  $\dot{h} \ll \text{Bo}$ . The second equation in Eq. (4) does not depend on  $h$  anymore. The droplet behaves as a simple forced oscillator, i.e.,  $\eta = c_6 \text{Bo} B(\omega) \Gamma \cos(\omega t + \phi) - \frac{c_6 \text{Bo}}{c_4}$ , where  $B(\omega)$  and  $\phi$  are trivially obtained. The resonance frequency related to this oscillator is given by

$$\omega_{\text{res}}^2 = \frac{c_4}{c_3 + c_6} \left[ 1 - \frac{c_4}{c_3 + c_6} \frac{\text{Oh}^2}{2} \right]. \quad (6)$$

To find  $h$  with the first equation of Eq. (4), it is convenient to define the amplitude  $H(t)$  of the thickness variation as  $h(t) = H(t) e^{c_2 c_6 \text{Bo} B(\omega) \Gamma \cos(\omega t + \phi)}$ . Calculations yield

$$\begin{aligned} \frac{3c_1 \mu_a \text{Oh}}{4\pi \rho \nu \text{Bo}} \frac{\dot{H}}{H^3} &= \{ \text{Bo} \Gamma [(c_4 - c_3 \omega^2) \cos(\omega t + \phi) \\ &\quad - c_5 \text{Oh} \omega \sin(\omega t + \phi)] \\ &\quad - 1 \} e^{2c_2 c_6 \text{Bo} B \Gamma \cos(\omega t + \phi)}. \end{aligned} \quad (7)$$

By integrating this equation over  $n$  periods ( $T = 2\pi/\omega$ ),

we obtain

$$H_{nT} = \left[ H_0^{-2} - \frac{8\pi\rho\nu\text{Bo}}{3c_1\mu_a\text{Oh}} CnT \right]^{-1/2} \quad (8)$$

where

$$\begin{cases} C = (c_4 - c_3\omega^2)B\Gamma I_1(2c_2c_6\text{Bo}B\Gamma) - I_0(2c_2c_6\text{Bo}B\Gamma) \\ I_k(x) = \frac{1}{\pi} \int_0^\pi e^{x\cos t} \cos(kt) dt \end{cases} \quad (9)$$

When  $C < 0$ , the averaged film thickness  $H$  decreases with time, and the droplet finally coalesces. Conversely, when  $C > 0$ ,  $H$  diverges: the solution is no longer valid. The droplet takes off,  $\dot{h}$  cannot be neglected anymore in Eq. (4), and bouncing occurs. The threshold acceleration for bouncing  $\Gamma_C$  can thus be defined as the value of  $\Gamma$  such that  $C = 0$ . This equation has one positive solution when  $c_4 - c_3\omega^2 > 0$ , and no solution in the other case. There is a cutoff frequency  $\omega_c^2 = \frac{c_4}{c_3}$  above which the model cannot predict bouncing ( $C$  is always negative). This frequency corresponds to the natural resonance of mode 2, when the droplet is directly excited (i.e., not through the air film dynamics). It is always higher than  $\omega_{\text{res}}$ , related to the forcing through the air film dynamics. Such a frequency was already observed in [9]. The curve  $\Gamma_C(\omega)$  tends asymptotically to a constant value  $>1$  when  $\omega \rightarrow 0$ . Moreover, when Oh is sufficiently small, a minimum in  $\Gamma_C$  is observed for a finite value of  $\omega$ , lower than  $\omega_{\text{res}}$  since  $\partial(B\Gamma_C)/\partial\omega > 0$  when  $\omega < \omega_c$ . Therefore, no minimum is observed when  $\omega_{\text{res}}$  is complex, i.e., when  $\text{Oh}^2 > 2(c_3 + c_6)/c_4$ .

In order to compare the model predictions to the experimental data shown in Fig. 1(a) to 1(d), a single fit has been made on coefficients  $c_2$ ,  $c_3$ ,  $c_5$ , and  $c_6$  ( $c_1$  is not present in Eq. (9) and  $c_4$  is fixed to 10). Obtained values ( $c_2, c_3, c_5, c_6$ )  $\simeq$  (25, 0.1, 3.3, 1) are similar to the values estimated theoretically (Table I). The comparison with experiments is acceptable, both qualitatively and quantitatively. In particular, the minima for low viscosities, and the divergence for high frequencies are reproduced. Quantitative discrepancies may be due to the fact that only mode 2 is considered in the modelling. The resonance occurs for a reduced frequency  $\omega_{\text{res}} < 3$  as long as  $\text{Oh} \lesssim 0.47$ . The cutoff reduced frequency for the mode 2 is  $\omega_c \simeq 10$ . For an oil droplet with  $R = 0.765$  mm bouncing in mode 2, resonance is observed at a maximum frequency of 51 Hz when the viscosity is less than 32 cSt, and the cutoff frequency of this mode is about 165 Hz. This is consistent with our experimental observations.

In conclusion, we have measured acceleration thresholds for bouncing droplets on a vertically vibrated high viscosity bath. The forcing frequency and the droplet vis-

cosity were varied. There is a cutoff frequency above which the droplet cannot use a mode 2 deformation to bounce. For low viscosity droplets, a minimum in the  $\Gamma_C(f)$  curve is observed, which corresponds to the resonance of the mode 2. In order to explain these features, a theoretical model was developed that includes both the deformation of the droplet and its influence on the film drainage. These effects are necessary in order to obtain periodic bouncing solutions such as those observed experimentally: the model is thus minimal. By varying four of the six constitutive coefficients of the model, it is possible to fit the experimental data.

T. G. and S. D. thank FRIA/FNRS for financial support. Exchanges between laboratories have been financially helped by the COST action P21. J.M. Aristoff (MIT), J.W. Bush (MIT), H. Caps (ULg), J.P. Lecomte (Dow Corning), and A. Bourlioux (U. Montreal) are acknowledged for fruitful discussions.

\*Tristan.Gilet@ulg.ac.be

†<http://www.grasp.ulg.ac.be>

- [1] H. A. Stone, A. D. Stroock, and A. Ajdari, *Annu. Rev. Fluid Mech.* **36**, 381 (2004).
- [2] T. Squires and S. R. Quake, *Rev. Mod. Phys.* **77**, 977 (2005).
- [3] D. L. Chen, L. Li, S. Reyes, D. N. Adamson, and R. F. Ismagilov, *Langmuir* **23**, 2255 (2007).
- [4] C. C. Cheng, C. A. Chang, and J. A. Yeh, *Opt. Express* **14**, 4101 (2006).
- [5] Y. Couder, E. Fort, C. H. Gautier, and A. Boudaoud, *Phys. Rev. Lett.* **94**, 177801 (2005).
- [6] Y. Couder, S. Protière, E. Fort, and A. Boudaoud, *Nature (London)* **437**, 208 (2005).
- [7] S. Protière, A. Boudaoud, and Y. Couder, *J. Fluid Mech.* **554**, 85 (2006).
- [8] S. Lieber, M. Hendershott, A. Pattanaporkratana, and J. Maclennan, *Phys. Rev. E* **75**, 056308 (2007).
- [9] T. Gilet, N. Vandewalle, and S. Dorbolo, *Phys. Rev. E* **76**, 035302(R) (2007).
- [10] D. Richard, C. Clanet, and D. Quéré, *Nature (London)* **417**, 811 (2002).
- [11] D. Legendre, C. Daniel, and P. Guiraud, *Phys. Fluids* **17**, 097105 (2005).
- [12] M. Kranz, K. Lunkenheimer, and K. Malysa, *Langmuir* **19**, 6586 (2003).
- [13] O. Reynolds, *Phil. Trans. R. Soc. Lond. A* **177**, 157 (1886).
- [14] L. Landau and E. Lifchitz, *Course on Theoretical Physics, 6-Fluid Mechanics* (Addison Wesley, Reading, MA, 1959).
- [15] E. Becker, W. Hiller, and T. Kowalewski, *J. Fluid Mech.* **231**, 189 (1991).
- [16] D. Terwagne, N. Vandewalle, and S. Dorbolo, *Phys. Rev. E* **76**, 056311 (2007).